Underwater Image Enhancement using Convolution Denoising Network and Blind Convolution

Shubhangi Adagale-Vairagar

CSMU, Navi Mumbai Mumbai, India | Department of AI&DS, Dr. D.Y. Patil Institute of Technology, Pimpri, India
vairagarss@gmail.com (corresponding author)

Praveen Gupta

Department of Computer Engineering, CSMU, Navi Mumbai Mumbai, India
Praveenymt2014@gmail.com

R. P. Sharma

Department of Computer Engineering, CSMU, Navi Mumbai Mumbai, India
sharmarpcsmu@gmail.com

ABSTRACT

Underwater Image Enhancement (UWIE) is essential for improving the quality of Underwater Images (UWIs). However, recent UWIE methods face challenges due to low lighting conditions, contrast issues, color distortion, lower visibility, stability and buoyancy, pressure and temperature, and white balancing problems. Traditional techniques cannot capture the fine changes in UWI texture and cannot learn complex patterns. This study presents a UWIE Network (UWIE-Net) based on a parallel combination of a denoising Deep Convolution Neural Network (DCNN) and blind convolution to improve the overall visual quality of UWIs. The DCNN is used to depict the UWI complex pattern features and focuses on enhancing the image's contrast, color, and texture. Blind convolution is employed in parallel to minimize noise and irregularities in the image texture. Finally, the images obtained at the two parallel layers are fused using wavelet fusion to preserve the edge and texture information of the final enhanced UWI. The effectiveness of UWIE-Net was evaluated on the Underwater Image Enhancement Benchmark Dataset (UIEB), achieving MSE of 23.5, PSNR of 34.42, AG of 13.56, PCQI of 1.23, and UCIQE of 0.83. The UWIE-Net shows notable improvement in the overall visual and structural quality of UWIs compared to existing state-of-the-art methods.

Keywords-blind convolution; deep convolutional neural network; image denoising; underwater image enhancement

I. INTRODUCTION

Underwater Images (UWIs) are used for various objectives in science, business, and pleasure. Marine research and biology, underwater environment monitoring, underwater archaeology, oceanography, fishery management, aquaculture, tourism, recreational scuba diving, underwater maintenance and inspection, underwater rescue and search operations, documentary and filmmaking productions, underwater vehicles, and commercial photography and advertising are among the most notable applications of UWIs [1-4].

UWIs are very difficult to work with due to their unique qualities and other difficulties compared to images captured above the water. UWIs often encounter problems due to color distortion, poor lighting, decreased vision, contrast issues, stability and buoyancy, pressure and temperature, white balance, and other issues [5-6]. The scattering and absorption processes are responsible for the color distortion, characterized by the primary impact on yellow and red objects and the tinting of green and blue colors. As a result of the haze that surrounds submerged objects, vision and overall UWI clarity are reduced [7]. The dispersion of light in the water also tends to affect the contrast. As water has a refractive index, the picture quality of a UWI may be compromised by blurring and distortion [8]. The restricted availability of UWI datasets makes it difficult to perform an exhaustive study [9]. Color distortion occurs due to differences in the water absorption rate for distinct wavelengths. The red color is absorbed earlier and the blue

color is absorbed later. Therefore, the blue color penetrates more deeply than the red color. Suspended particles in the water, such as sediments and plankton, scatter light and result in reduced visibility, a foggy effect, and poor contrast [10-11]. Stability is negatively affected by buoyant forces, making it challenging to capture stable images, causing a lack of sharpness and motion blur. In deep water, the temperature decreases and water pressure increases, degrading light behavior and reducing image clarity. The light-bending effect in water leads to the creation of haze and bright spots [12-13]. Figure 1 visualizes various issues associated with UWIs.
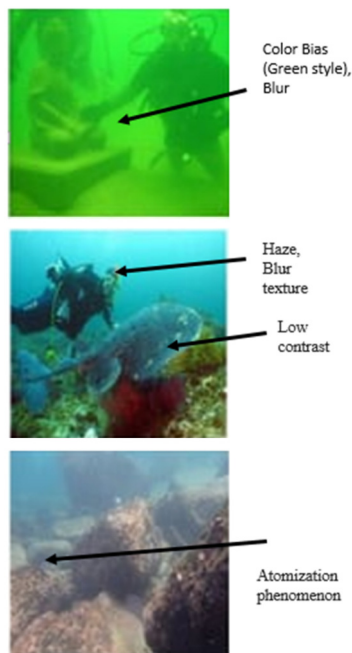

Fig. 1.   Several characteristics of UWIs.

UWIs suffer from low contrast and color cast due to distance, wavelength-based scattering, and attenuation. In [14], UColor was proposed, which is a combination of a multicolor space encoder network and an attention mechanism for UWIE. A multicolor space encoder was utilized to characterize distinct colors in a unified structure, and an attention mechanism was used to integrate and highlight multicolor attributes. This method showed superior results for contrast enhancement and color cast adaptation but gave inferior results for UWIs with lower illumination. In [15], the Bayesian Retinex (BR) method was presented for UWIE, focusing on the multicolor gradient priors of illumination and reflectance. The BR scheme has shown naturalness preservation, color correction, structure and detail promotion, and noise and artifact minimization. In [16], a robust, efficient, generalized, and fast UWIE method was proposed, called Minimal Color Loss and Locally Adaptive Contrast Enhancement (MLLE), providing superior performance in sandstorm and foggy environments. This method used a locally adaptive color correction technique based on the minor color loss principle and the highest attenuation map-guided fusion strategy. It also provided a locally adaptive contrast enhancement scheme that uses

integral and squared integral maps to competently calculate the variance and mean of local UWI blocks for contrast adjustment. In [17], an innovative approach was proposed, utilizing a random forest regression model to evaluate the transmission of underwater scenes. Building on this, in [18], a technique was designed to restore UWIs leveraging principles of light absorption and addressing image blurriness. In [19], an advanced method employing a Generalized Dark Channel Prior (GDCP) framework was proposed, specifically designed to rectify underwater, foggy, and affected by haze and sandstorm images. This method marked a significant advance in image enhancement and restoration techniques, offering potential applications in various domains such as marine exploration, environmental monitoring, and remote sensing. In [20], a UWI restoration technique based on an adaptive attenuation-curve prior was introduced. In [21], a UWI restoration approach was presented, which focused on estimating transmission maps and decomposing reflections. DL-based schemes based on DCNN and generative adversarial networks have attracted wide attention toward UWIE due to their high-level hierarchical feature learning and ability to handle multiple issues at once [22-23]. However, several problems make UWI analysis and object recognition difficult. As water bodies scatter and absorb incoming light, underwater images are blue-green or fog-like. Blur, poor contrast, atomization phenomena, noise, color distortion, restricted visual range, uneven lighting, color bias, and ambiguous details are common factors that reduce the quality of UWIs. Thus, improving UWIs while preserving picture-perceived quality is difficult [24-25]. This study presents a robust method, called UWIE-Net, based on a parallel DCNN and blind convolution-based denoising schemes. The main contributions of this study are summarized as follows:

- The DCNN-based UWIE enhances the contrast, color, and texture of the image.

- Blind convolution-based image denoising minimizes the noise and irregularities in the image texture.

- Discrete Wavelet Transform (DWT)-based image fusion improves the edge and texture information of the UWIs.

II.   METHODOLOGY

Figure 2 presents the flow diagram of the proposed method, which uses in parallel a DCNN and a blind convolution model to denoize the image. DCNN enhances the contrast, color, and texture of the image. The blind convolution is employed to minimize the noise and irregularities in the image's texture. The color UWI is divided into three color channels: red (RC), green (GC), and blue (BC). The DCNN and blind convolution-based denoising are applied to three color components separately to analyze the effect of color variation on the UWI. The images obtained from the DCNN and blind convolution are fused using mean wavelet fusion to obtain the overall enhanced UWI. Wavelet-based fusion helps retain the structural, textural, and edge information of UWIs. The hybrid combination of blind convolution and DCNN provides superior generalization capability and a lightweight DL-based UWI framework that can minimize color distortion/blur, color unbalancing, scattering and absorption effect, noise, irregularities, haze, and contrast issues cumulatively.

TABLE I.   COMPARATIVE ANALYSIS OF STUDIES ON UWIE

| Study	Method	Dataset	Performance	Remarks
[14]	UColor	Test-S1000 Test-R90	Test-S1000 (PSNR-23.05, MSE-0.50), Test-R90 (PSNR-20-63, MSE-0.73)	Poor results for UWIs with limited lightning.
[16]	MLLE	UIEB, UCCS, UIQS	UIEB (AG-1227, PCQI-1.136, UIQM-5.29, CCF-46.872) UIEB (AG-10.121, PCQI-1.203, UIQM-3.915, CCF-41.707), UIQS (AG-10.505, PCQI-1.180,UIQM-3.928, CCF-44.201)	Good generalization capability, better contrast enhancement, etc. Fails to handle UWIs captured under low illumination conditions.
[7]	GLHDF	UIEB	MSE=87.31, SNR=27.39, AG=9.85, PCQI=0.94 , UCIQUE=0.67	Better results for color disturbance, less visual quality of UWIs.
[17]	Hybrid based UWIE	UIEB	MSE=88.34, SNR=26.35, AG=8.98, PCQI=0.93, UCIQUE=0.65	Poor AG, subjected to poor illumination variations, complexity in techniques.
[18]	UIBLA	UIEB	MSE=83.14, PSNR=28.50, AG=8.23, PCQI=0.94, UCIQUE=0.68	Poor AG, fails to maintain the structural similarity of underwater objects.
[19]	GDCP	UIEB	MSE=78.03, SNR=29.20, AG=9.25, PCQI=0.94, UCQUE=0.72	Good PCQI and UCQUE, has vast impact of poor color correction, edge smoothening, and blurring.
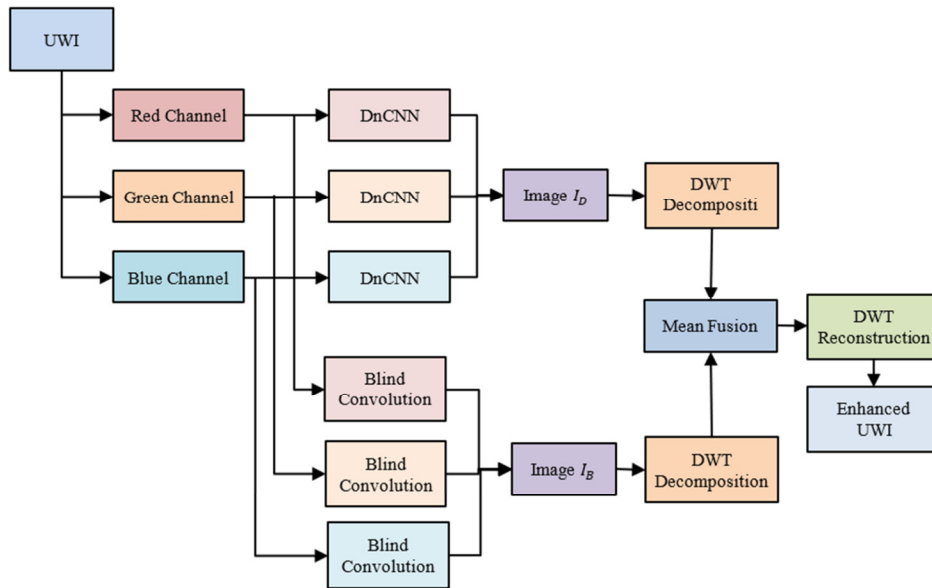
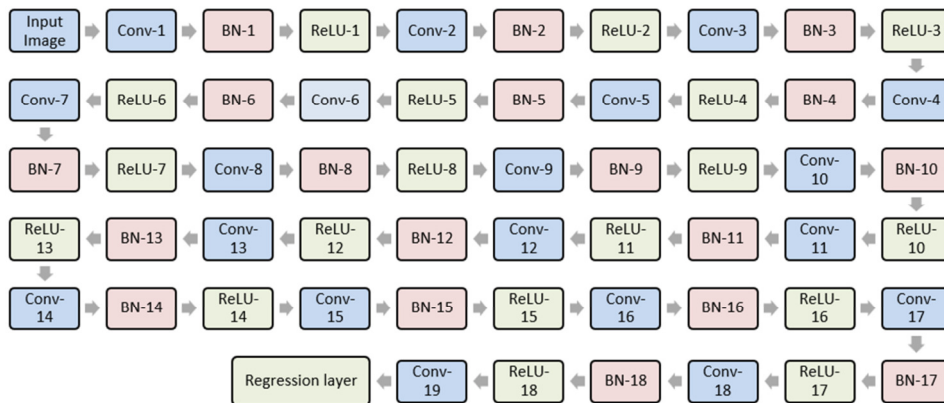Fig. 2.   Flow diagram of the proposed UWIE scheme.

Fig. 3.   DCNN framework.

A. DCNN

The DCNN consists of 20 convolution layers, 19 Batch Normalization layers (BN), 19 Rectified Linear Unit layers (ReLU), and one regression layer. It uses a series combination of convolution layers followed by the ReLU and BN layers.

Figure 2 shows the architecture of the DCNN. The convolution process (IC) is given in (1), where the input image (im) is convolved with the convolution filter (K) [27-28].

$$IC(x,y) = \sum_{i=1}^{r} \sum_{y-1}^{c} im(i-x, j-y).K(x,y) \quad (1)$$

The ReLU layer (R) boosts the non-linearity of the convolution features to enhance the quality of features. It replaces the negative values with zero [27-28]:

$$R(x, y) = max(0, IC(x, y)) \qquad (2)$$

The BN layer standardizes the ReLU layer output to enhance the training performance using the mean (μ), standard deviation (σ), scale (α), and offset (β) parameters as given in (3). The values are normalized for the batch size of 32 [27-28].

$$BN = \propto.\frac{R-\mu}{\sigma} + \beta \qquad (3)$$

B. Blind Convolution

Blind convolution-based image denoising is utilized to improve the quality of noise-corrupted UWIs. This technique works by repeatedly estimating the blur kernel that causes the UWI deterioration and the latent clean UWI. Blind convolution-based algorithms are very flexible to various noise circumstances since they dynamically infer the blur kernel, unlike classic denoising approaches that assume a predetermined degradation model. These techniques can remove noisy artifacts caused by convolution with an unknown kernel and efficiently recover the underlying UWI structure using sophisticated mathematical formulations such as variational models or deep learning architectures. Blind convolution-based denoising algorithms use iterative optimization approaches to achieve a compromise between noise reduction and feature preservation, leading to high-fidelity UWI restorations that are aesthetically pleasant and applicable to a wide range of real-world scenarios.

C. DWT-based Fusion

DWT-based fusion is used to preserve the content of UWIs. The outputs of the DCNN and blind convolution-based enhancement schemes are decomposed using DWT into four components, representing the approximation, horizontal, detailed, and vertical components of UWIs. The mean fusion is applied to every decomposition part of DWT to retain the textural, structural, and edge information of UWIs. The output of DCNN (I_D) and Blind convolution (I_B) is decomposed using the wavelet Daubechies filter (db2) as given in (4) and (5). Here, AD, VD, HD, and DD denote the approximation, vertical, horizontal, and detailed components of the J-level decomposition of the DCNN denoised image. In addition, AB, VB, HB, and DB describe the approximation, vertical, horizontal, and detailed components of the blind convolution output. Two-level wavelet decomposition ($J = 2$) was used to decompose the images to get finer details of UWIs.

$$DWT(I_D) = \{AD_j, VD_j, HD_j, DD_j\}_{j=1}^{J} \qquad (4)$$

$$DWT(I_B) = \{AB_j, VB_j, HB_j, DB_j\}_{j=1}^{J} \qquad (5)$$

The mean of the approximation (A_m), vertical (V_m), horizontal (H_m), and detailed (D_m) components are calculated using:

$$A_m = \frac{AD+AB}{2} \qquad (6)$$

$$V_m = \frac{VD+VB}{2} \qquad (7)$$

$$H_m = \frac{HD+HB}{2} \qquad (8)$$

$$D_m = \frac{DD+DB}{2} \qquad (9)$$

The final enhanced image is obtained using inverse DWT as given by:

$$Enhanced_{Image} = IDWT(A_m, V_m, H_m, D_m\} \qquad (10)$$

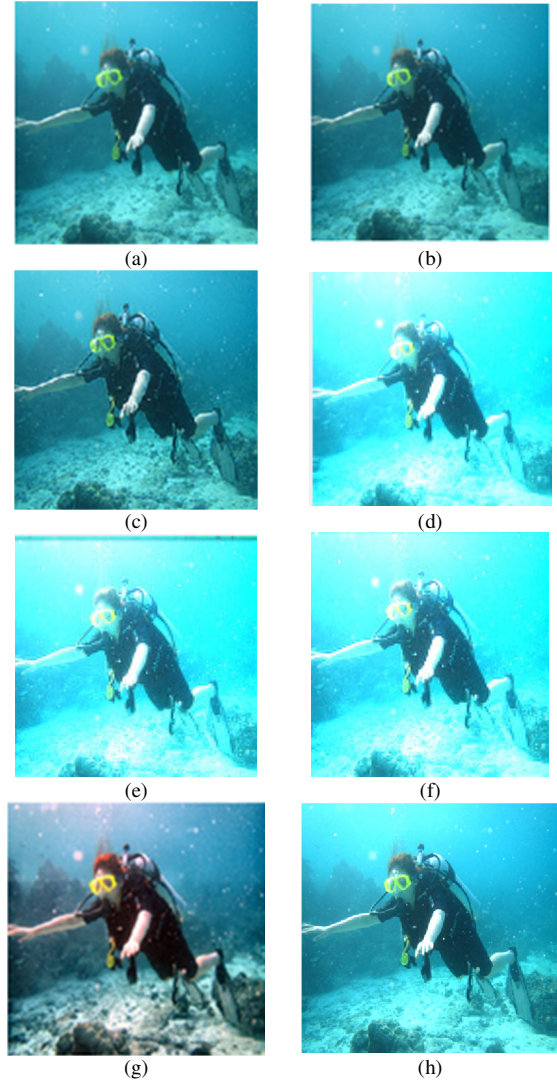Figure 4 shows the results of the DWT-based fusion.

Fig. 4.   Stepwise results for the proposed UWIE scheme: (a) Original UWIE, (b) DnCNN output, (c) Blind convolution output, (d) DWT decomposition of DnCNN output (2nd level), (e) DWT decomposition of blind convolution output (2nd level), (f) Fusion of DWT decomposition, (g) Reference UWI, (h) Enhanced UWI.

III.   EXPERIMENTAL RESULTS AND DISCUSSIONS

The proposed system was implemented using MATLAB R2023b on a PC with 20GB RAM and 2 GB graphics card in a Windows environment. The UIEB dataset consists of 950 UWIs where 890 of them have a reference image [26]. It

includes images with different scattering, low contrast, color bias, atomization phenomenon, blur, unclear details, and noise levels.

A. Evaluation Metrics

The performance of the proposed UWIE was evaluated based on MSE, PSNR, AG, PCQI, and UCIQI. MSE offers an overall quantitative error measure between the reference (R) and the enhanced UWI (U) as given in (11), measuring the overall change in the UWI texture and color properties. PSNR provides the overall visual quality measure of the UWIE, which depends on the MSE value (12). A higher PSNR value indicates the preservation of the visual quality and information of UWIs. The AG measures the average value of all pixels on a UWI gradient map, which imitates the features of exhaustive texture variations and the clarity of the UWI. The AG depicts the variations over the edges of UWIs, measuring the changes made to the horizontal and vertical edges of the images. Higher values indicate the preservation of edge information and the

structure of image objects. The larger the average gradient value, the richer the UWI level and the more precise the UWI. AG is given by (13) where $\frac{\partial E}{\partial x}$ and $\frac{\partial E}{\partial x}$ stand for the average horizontal and vertical gradients of UWIs.
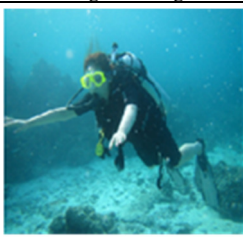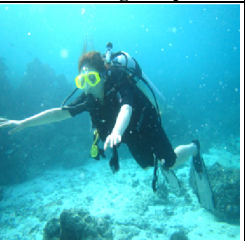
$$MSE = \frac{1}{Row*Col}\sum_{x=1}^{Row}\sum_{y=1}^{Col}(E(x,y) - R(x,y))^2 \quad (11)$$

$$PSNR = \frac{2^b - 1}{\sqrt{MSE}} \qquad (12)$$

$$AG = \frac{1}{Row*Col}\sum_{x=1}^{Row}\sum_{y=1}^{Col}\sqrt{\frac{\left(\frac{\partial E}{\partial x}\right)^2 + \left(\frac{\partial E}{\partial y}\right)^2}{2}} \qquad (13)$$

PCQI offers a measure of color distortion and color fidelity. It indicates the preservation of color properties in the reference image. The UCIQE provides evaluation metrics to measure poor visibility, color distortion, and contrast issues. A higher value of UCIQE indicates better visibility, reduced color distortions, and enhanced contrast.

TABLE II.   VISUALIZATION OF RESULTS FOR UIEB DATASET SAMPLE 1

	Original Image	DCNN output	Blind Convolution Output	Final image output
RBG Image				
Red Channel				
Green Channel				
Blue Channel				

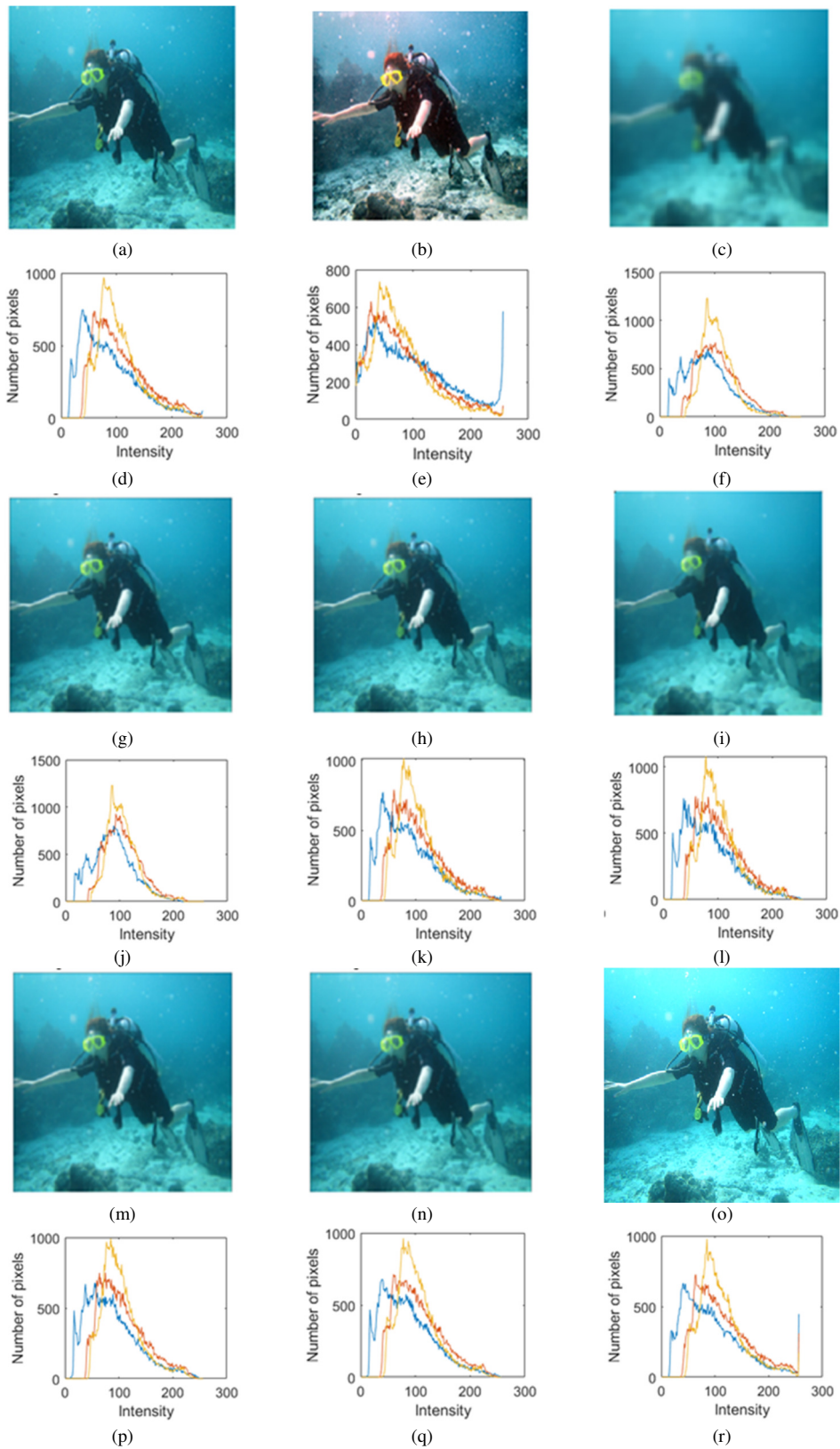Fig. 5.   Comparative results of the proposed method: (a) Original Image, (b) Reference Image, (c) Gaussian filter, (d-f) Histograms for original, reference, and Gaussian filter, (g) Median Filter (h) Weiner Filter (i) Wavelet filter, (j-l) Histograms of median, Weiner and wavelet filters, (m) DCNN, (n) Blind convolution, (o) DCNN+blind Convolution (p-r) histograms for DCNN+blind convolution.

B. Results and Discussions

Table II provides the results for the samples from the UIEB dataset, showing the results for DCNN-based denoising, blind convolution-based denoising, and enhanced UWIs. The proposed UWIE scheme provides better visual quality for UWIs affected by color disparity, poor contrast, color distortion, lower visibility, stability and buoyancy, pressure and temperature, and white balancing problems. The results of combining DCNN and blind convolution were superior compared to those of the individual methods.

The effectiveness of the proposed UWIE-Net was compared with the results of several traditional UWIE techniques such as the Gaussian filter, median filter, Weiner filter, and wavelet filter, as shown in Figure 5. The histograms of the enhanced images using different techniques show the distribution of the red, green, and blue intensities in the enhanced UWI. The proposed method combining DCNN and blind convolution showed better visual and perceptual image quality. The histograms of the proposed enhanced UWI and reference showed a lower disparity (8%) than the traditional techniques (15-34%).

Table III compares the results of the proposed with traditional popular UWIE techniques for the sample UWI. The proposed method achieved PSNR of 41.53, MSE of 37.70, AG of 11.34, PCQI of 0.99, and UCIQE of 0.87, which is superior to traditional techniques. The DCNN and blind convolution alone offered PSNR of 40.32 and 41.1 which indicate superior visual quality compared to wavelet, Weiner, median, and Gaussian filters.

TABLE III.   RESULTS FOR UIEB SAMPLE

Algorithm	MSE	PSNR	AG	PCQI	UCIQE
Gaussian	41.7	39.49	3.78	0.98	0.73
Median	41.3	39.68	4.71	0.98	0.74
Weiner	41.1	39.78	5.07	0.9	0.76
Wavelet	40.8	39.92	7.01	0.93	0.76
DnCNN	40	40.32	7.9	0.99	0.83
Blind Convolution	38.5	41.1	9.06	0.99	0.84
DnCNN+ Blind Convolution	**37.7**	**41.53**	11.34	**0.99**	0.87

The overall results for the UIEB dataset are summarized in Table IV. The proposed denoising scheme achieved MSE of 23.5, PSNR of 34.42, AG of 13.56, PCQI of 1.23, and UCIQE of 0.83, which is a notable improvement over the results of DCNN and blind convolution. The DCNN-based UWIE scheme provided an MSE of 35.6, PSNR of 32.61, AG of 12.78, PCQI of 1.18, and UCIQE of 0.80. The blind convolution-based UWIE scheme resulted in an MSE of 30.6, PSNR of 33.27, AG of 13.13, PCQI of 1.19, and UCIQE of 0.81. UWIE-Net provided an overall boost of 33.98% in MSE, 5.55% in PSNR, 6.10% in AG, 4.23% in PCQI, and 3.75% in UCIQE over DCNN-based UWIE. In addition, UWIE-Net offered an overall improvement of 23.20%, 34.42%, 13.56%, 3.36%, and 2.46% in MSE, PSNR, AG, PCQI, and UCIQE over blind-convolution-based UWIE. The DCNN can learn the complex pattern features of UWIs, retain the fine details of the UWIs, and is robust against different noises. Blind convolution-based UWIE provides robustness for unknown noise, turbidity, camera artifacts, and lighting conditions and

preserves fine details of the UWI texture. The proposed UWIE-Net combines blind convolution and DCNN to enhance the robustness of the UWIE under different conditions. The proposed scheme provides superior AG, PCQU, and UCIQE due to better quality texture, edge smoothness, and color correction by combining the advantages of both methods.

Table IV and Figures 6-10 compare several UWIE techniques, showing significant variations. In contrast to other approaches, the GLHDF method had the highest MSE score of 87.31, suggesting relatively low fidelity. The proposed method had the lowest MSE of 23.5, indicating better preservation of image quality. The comparison shows significant differences in PSNR values. The proposed method had the highest PSNR of 34.42, indicating the best reconstruction quality. In addition, the proposed method regularly outperformed the other approaches, in AG, PCQI, and UCIQE, demonstrating significant differences. The statistical analysis and comparison highlights how the proposed method produces better image restoration results, defined by reduced error metrics and higher quality indicators.

TABLE IV.   PERFORMANCE COMPARISON ON THE UIEB DATASET

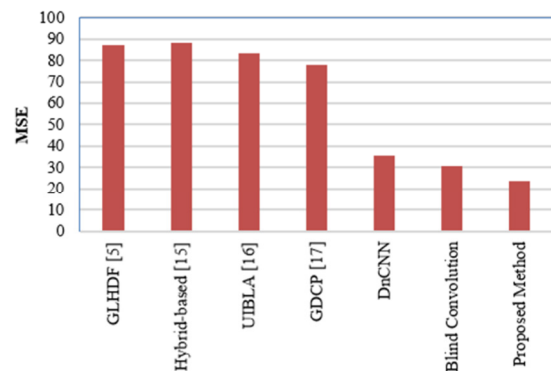| Method	MSE	PSNR	AG	PCQI	UCIQE
GLHDF [5]	87.31	27.39	9.85	0.94	0.67
Hybrid-based [15]	88.34	26.35	8.98	0.93	0.65
UIBLA [16]	83.14	28.50	8.23	0.94	0.68
GDCP [17]	78.03	29.20	9.25	0.94	0.72
DnCNN	35.6	32.61	12.78	1.18	0.80
Blind Convolution	30.6	33.27	13.13	1.19	0.81
Proposed Method	23.5	34.42	13.56	1.23	0.83

Fig. 6.   MSE comparison of UWIE techniques.
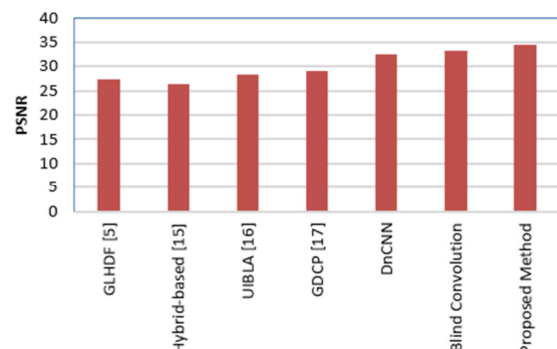

Fig. 7.   PSNR comparison of UWIE techniques.
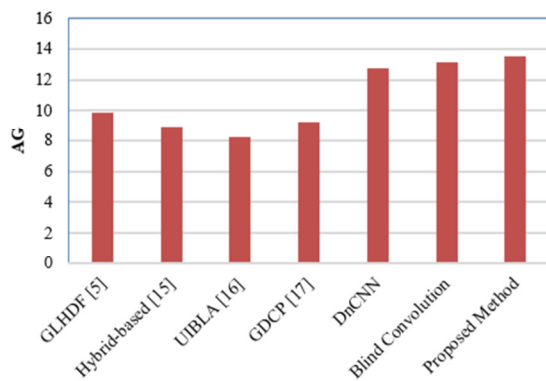
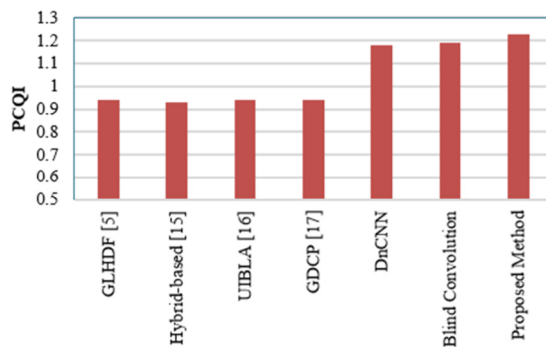Fig. 8.   AG comparison of UWIE techniques.

Fig. 9.   PCQI comparison of UWIE techniques.
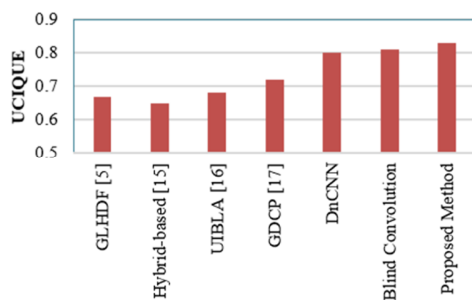

Fig. 10.   UCIQUE comparison of UWIE techniques.

The DCNN has 669,505 trainable parameters. The proposed method required an average enhancing time of 5 seconds.

IV.   CONCLUSION AND FUTURE SCOPE

The proposed method enhances UWIs by combining DCNN and blind convolution. DCNN focuses on improving the image's contrast, color, and texture. The blind convolution is used in parallel to help in minimizing the noise and irregularities in the image texture. The proposed hybrid DL-based denoising framework provided superior generalization capability that deals with different issues in UWIs, such as color distortion, noise, scattering, color imbalance, absorption, etc. It is a lightweight DL-based framework that helps preserve the structural, perceptual, and visual quality of UWIs. This enhancement method helps to learn the local characteristics of UWIs to minimize abnormalities. The proposed method provided superior image quality compared to previous ML-

based schemes, achieving overall overall MSE of 23.5, PSNR of 34.42, AG of 13.56, PCQI of 1.23, and UCIQE of 0.81 on the UIEB dataset. The proposed UWIE-Net provides an imperative boost of 23-73% in MSE, 3-26% in PSNR, 3-28% in AG, 3-31% in PCQI, and 2-24% in UCIQE over traditional UWIE methods.

In the future, the proposed scheme can be improved to provide a generalized framework for all types of UWI enhancement. The complexity of the DL frameworks can be minimized by utilizing hyperparameter tuning and learning optimization of the DL frameworks. In addition, the system can be extended for underwater image and object segmentation.

REFERENCES

[1]   S. Raveendran, M. D. Patil, and G. K. Birajdar, "Underwater image enhancement: a comprehensive review, recent trends, challenges and applications," *Artificial Intelligence Review*, vol. 54, no. 7, pp. 5413–5467, Oct. 2021, https://doi.org/10.1007/s10462-021-10025-z.

[2]   H. T. R. Kurmasha, A. F. H. Alharan, C. S. Der, and N. H. Azami, "Enhancement of Edge-based Image Quality Measures Using Entropy for Histogram Equalization-based Contrast Enhancement Techniques," *Engineering, Technology & Applied Science Research*, vol. 7, no. 6, pp. 2277–2281, Dec. 2017, https://doi.org/10.48084/etasr.1625.

[3]   S. Rani, Y. Chabrra, and K. Malik, "An Improved Denoising Algorithm for Removing Noise in Color Images," *Engineering, Technology & Applied Science Research*, vol. 12, no. 3, pp. 8738–8744, Jun. 2022, https://doi.org/10.48084/etasr.4952.

[4]   M. K. Moghimi and F. Mohanna, "Real-time underwater image enhancement: a systematic review," *Journal of Real-Time Image Processing*, vol. 18, no. 5, pp. 1509–1525, Oct. 2021, https://doi.org/10.1007/s11554-020-01052-0.

[5]   J. Zhou *et al.*, "UGIF-Net: An Efficient Fully Guided Information Flow Network for Underwater Image Enhancement," *IEEE Transactions on Geoscience and Remote Sensing*, vol. 61, pp. 1–17, 2023, https://doi.org/10.1109/TGRS.2023.3293912.

[6]   M. Yang, K. Hu, Y. Du, Z. Wei, Z. Sheng, and J. Hu, "Underwater image enhancement based on conditional generative adversarial network," *Signal Processing: Image Communication*, vol. 81, Feb. 2020, Art. no. 115723, https://doi.org/10.1016/j.image.2019.115723.

[7]   L. Bai, W. Zhang, X. Pan, and C. Zhao, "Underwater Image Enhancement Based on Global and Local Equalization of Histogram and Dual-Image Multi-Scale Fusion," *IEEE Access*, vol. 8, pp. 128973–128990, 2020, https://doi.org/10.1109/ACCESS.2020.3009161.

[8]   X. Chen, P. Zhang, L. Quan, C. Yi, and C. Lu, "Underwater Image Enhancement based on Deep Learning and Image Formation Model." arXiv, Jan. 07, 2021, https://doi.org/10.48550/arXiv.2101.00991.

[9]   D. Zhang *et al.*, "Robust underwater image enhancement with cascaded multi-level sub-networks and triple attention mechanism," *Neural Networks*, vol. 169, pp. 685–697, Jan. 2024, https://doi.org/10.1016/j.neunet.2023.11.008.

[10]   C. W. Park and I. K. Eom, "Underwater image enhancement using adaptive standardization and normalization networks," *Engineering Applications of Artificial Intelligence*, vol. 127, Jan. 2024, Art. no. 107445, https://doi.org/10.1016/j.engappai.2023.107445.

[11]   J. Wen *et al.*, "WaterFormer: A Global–Local Transformer for Underwater Image Enhancement With Environment Adaptor," *IEEE Robotics & Automation Magazine*, vol. 31, no. 1, pp. 29–40, Mar. 2024, https://doi.org/10.1109/MRA.2024.3351487.

[12]   X. Liu, Z. Gu, H. Ding, M. Zhang, and L. Wang, "Underwater Image Super-Resolution Using Frequency-Domain Enhanced Attention Network," *IEEE Access*, vol. 12, pp. 6136–6147, 2024, https://doi.org/10.1109/ACCESS.2024.3351730.

[13]   B. Sun, Y. Mei, N. Yan, and Y. Chen, "UMGAN: Underwater Image Enhancement Network for Unpaired Image-to-Image Translation," *Journal of Marine Science and Engineering*, vol. 11, no. 2, Feb. 2023, Art. no. 447, https://doi.org/10.3390/jmse11020447.

[14] C. Li, S. Anwar, J. Hou, R. Cong, C. Guo, and W. Ren, "Underwater Image Enhancement via Medium Transmission-Guided Multi-Color Space Embedding," *IEEE Transactions on Image Processing*, vol. 30, pp. 4985–5000, 2021, https://doi.org/10.1109/TIP.2021.3076367.

[15] P. Zhuang, C. Li, and J. Wu, "Bayesian retinex underwater image enhancement," *Engineering Applications of Artificial Intelligence*, vol. 101, May 2021, Art. no. 104171, https://doi.org/10.1016/j.engappai.2021.104171.

[16] W. Zhang, P. Zhuang, H. H. Sun, G. Li, S. Kwong, and C. Li, "Underwater Image Enhancement via Minimal Color Loss and Locally Adaptive Contrast Enhancement," *IEEE Transactions on Image Processing*, vol. 31, pp. 3997–4010, 2022, https://doi.org/10.1109/TIP.2022.3177129.

[17] C. Li, J. Guo, C. Guo, R. Cong, and J. Gong, "A hybrid method for underwater image correction," *Pattern Recognition Letters*, vol. 94, pp. 62–67, Jul. 2017, https://doi.org/10.1016/j.patrec.2017.05.023.

[18] Y. T. Peng and P. C. Cosman, "Underwater Image Restoration Based on Image Blurriness and Light Absorption," *IEEE Transactions on Image Processing*, vol. 26, no. 4, pp. 1579–1594, Apr. 2017, https://doi.org/10.1109/TIP.2017.2663846.

[19] Y. T. Peng, K. Cao, and P. C. Cosman, "Generalization of the Dark Channel Prior for Single Image Restoration," *IEEE Transactions on Image Processing*, vol. 27, no. 6, pp. 2856–2868, Jun. 2018, https://doi.org/10.1109/TIP.2018.2813092.

[20] Y. Wang, H. Liu, and L.-P. Chau, "Single Underwater Image Restoration Using Adaptive Attenuation-Curve Prior," *IEEE Transactions on Circuits and Systems I: Regular Papers*, vol. 65, no. 3, pp. 992–1002, Mar. 2018, https://doi.org/10.1109/TCSI.2017.2751671.

[21] M. Yang, A. Sowmya, Z. Wei, and B. Zheng, "Offshore Underwater Image Restoration Using Reflection-Decomposition-Based Transmission Map Estimation," *IEEE Journal of Oceanic Engineering*, vol. 45, no. 2, pp. 521–533, Apr. 2020, https://doi.org/10.1109/JOE.2018.2886093.

[22] D. Berman, D. Levy, S. Avidan, and T. Treibitz, "Underwater Single Image Color Restoration Using Haze-Lines and a New Quantitative Dataset," *IEEE Transactions on Pattern Analysis and Machine Intelligence*, vol. 43, no. 8, pp. 2822–2837, Dec. 2021, https://doi.org/10.1109/TPAMI.2020.2977624.

[23] Y. Zhou, Q. Wu, K. Yan, L. Feng, and W. Xiang, "Underwater Image Restoration Using Color-Line Model," *IEEE Transactions on Circuits and Systems for Video Technology*, vol. 29, no. 3, pp. 907–911, Mar. 2019, https://doi.org/10.1109/TCSVT.2018.2884615.

[24] D. Akkaynak and T. Treibitz, "Sea-Thru: A Method for Removing Water From Underwater Images," in *2019 IEEE/CVF Conference on Computer Vision and Pattern Recognition (CVPR)*, Long Beach, CA, USA, Jun. 2019, pp. 1682–1691, https://doi.org/10.1109/CVPR.2019.00178.

[25] K. Iqbal, M. Odetayo, A. James, Rosalina Abdul Salam, and Abdullah Zawawi Hj Talib, "Enhancing the low quality images using Unsupervised Colour Correction Method," in *2010 IEEE International Conference on Systems, Man and Cybernetics*, Istanbul, Turkey, Oct. 2010, pp. 1703–1709, https://doi.org/10.1109/ICSMC.2010.5642311.

[26] C. Li *et al.*, "An Underwater Image Enhancement Benchmark Dataset and Beyond," *IEEE Transactions on Image Processing*, vol. 29, pp. 4376–4389, 2020, https://doi.org/10.1109/TIP.2019.2955241.

[27] K. B. Bhangale and M. Kothandaraman, "Survey of Deep Learning Paradigms for Speech Processing," *Wireless Personal Communications*, vol. 125, no. 2, pp. 1913–1949, Jul. 2022, https://doi.org/10.1007/s11277-022-09640-y.

[28] K. Bhangale and M. Kothandaraman, "Speech Emotion Recognition Based on Multiple Acoustic Features and Deep Convolutional Neural Network," *Electronics*, vol. 12, no. 4, Jan. 2023, Art. no. 839, https://doi.org/10.3390/electronics12040839.